Building and Environment 181 (2020) 107120

Contents lists available at ScienceDirect

Building and Environment

journal homepage: http://www.elsevier.com/locate/buildenv

The effect of exhaust emissions from a group of moving vehicles on pollutant dispersion in the street canyons

Tianhao Shi [a], Tingzhen Ming [a,*], Yongjia Wu [a], Chong Peng [b], Yueping Fang [c,**], Renaud de_Richter [d]

[a] School of Civil Engineering and Architecture, Wuhan University of Technology, Wuhan, 430070, China
[b] School of Architecture and Urban Planing, Huazhong University of Science and Technology, Wuhan, 430074, China
[c] Centre for Research in the Built and Natural Environment, School of Energy, Construction and Environment, Coventry University, Priory Street, CV1 5FB, Coventry, UK
[d] Tour-Solaire.Fr, 8 Impasse des Papillons, F34090, Montpellier, France

ARTICLE INFO

Keywords:
Vehicular exhaust
Street canyon
Vehicle-induced turbulence
Pollution dispersion
Vehicle arrangement
Personal intake fraction (P_IF)

ABSTRACT

Moving vehicles are the primary emission source of road pollution and the vehicle-induced turbulence (VIT) affecting the flow field in the street canyon. This paper used the dynamic mesh updating method to simulate the air pollution under the real situation of vehicle movement and exhaust emission in the street canyon. The dispersion characteristics of vehicular exhaust under various vehicle arrangements were analyzed. The personal intake fraction (P_IF) was introduced as an index to analyze the impact of factors such as vehicle speed and ambient wind velocity on the pollution exposure level of pedestrians. Based on the general assumptions in the study of street canyon pollution that vehicle-induced turbulence (VIT) is a continuous turbulence source and vehicle exhaust pollutants is a uniform pollution source, the conditions of the hypothesis are preliminarily explored. The research indicates that VIT can be regarded as a continuous turbulence source when vehicles maintain a "safe distance" on the road and form a stable traffic flow. Moreover, according to the range of dispersion of exhaust pollution, a "healthy distance" was proposed to guide driver to avoid direct impact of exhaust emitted from the vehicles in front.

1. Introduction

In modern society, people's daily life is increasingly dependent on cars. According to the data published by the National Bureau of Statistics of China, at the end of 2019, China had over 260 million motor vehicles on the road, including 220 million private cars [1]. The dramatic increase of vehicles on the road has caused serious environmental pollution although the swift speed of vehicles makes people's daily life easier. For example, large numbers of vehicles consume large quantities of petroleum resources. Meanwhile, vehicles exhaust emissions become the principal source of urban air pollution [2]. The acceleration of urbanization has led to a vast influx of people into cities, and the shortage of per capita living and office space has prompted people to build higher buildings to maximize the use of land. Towering buildings and narrow streets formed the typical structure of a city - street canyon. Due to the continuing increase of exhaust emission of vehicles on the road and the blocking effect of tall buildings on the dispersion of pollutants, street canyons have become the most polluted places in the city [3]. In recent years, the street canyon has attracted worldwide attention because of its special air pollution patterns. Methods such as field measurement [4], wind tunnel experiment [5] and numerical simulation [6,7] are used to study the pollution distribution characteristics in the street canyon.

It is generally believed that the turbulence and mean flow are the main factors affecting the diffusion of pollution in the street canyon, particularly the turbulence [8]. Street canyon geometry, such as aspect ratio [9–13], viaducts [14,15], green plants [16,17] and wind catchers [18,19] are the impact factors of the vortex structure of the flow field in the street canyon. Generally speaking, with the aspect ratio increasing, the pollutant dispersion capacity decreases, and the air pollution intensifies [20]. Gromke [21] found that when the ambient wind is perpendicular to the street canyon, planting trees causes increased concentrations of pollutants near the leeward walls and dropped concentrations of pollutants near the windward. The wind catcher can introduce external wind into the street canyon, which is conducive to the dispersion of pollution [19]. After the street canyon geometry is

* Corresponding author.
** Corresponding author.
E-mail addresses: tzming@whut.edu.cn (T. Ming), ac1179@coventry.ac.uk (Y. Fang).

https://doi.org/10.1016/j.buildenv.2020.107120
Received 15 May 2020; Received in revised form 6 July 2020; Accepted 8 July 2020
Available online 23 July 2020

Nomenclature

α	ground roughness index
U_*	friction velocity
U_{ref}	wind velocity at the reference height
z_{ref}	reference height
ν	kinematic viscosity
δ_{ij}	Kronecker delta
Γ	diffusion coefficient
ρ	air density
$\overline{u_L' u_J'}$	Reynolds stress term
$\overrightarrow{u_g}$	grid speed of the moving mesh
t	time
U_i	the average speed components in the i-th directions
U_j	the average speed components in the j-th directions
ε	Dissipation rate of turbulent kinetic energy
ν_t	turbulent viscosity coefficient
D	mass diffusion coefficient
κ	Turbulent kinetic energy
$\frac{dV}{dt}$	first-order time derivative of the control volume
$\overrightarrow{u}$	velocity vector of the fluid
$\overline{u_l}$	von Karman constant

determined, the meteorological conditions will affect the street canyon flow field, including the ambient wind and solar radiation, which are in the form of thermal-induced turbulence (TIT) and wind-induced turbulence (WIT) respectively. Existing researches have shown that the wind direction [22,23] determines the transmission direction of vehicle pollutants, and the wind force [24,25] determines the dilution degree of pollutants. Solar radiation causes uneven temperatures of the ground and the buildings on both sides of the street canyon. The study [26] found that a high temperature on the windward side is conductive to the diffusion of pollution, while the high temperature on the leeward side seriously hinders the diffusion of pollution.

In real street canyons, the movement of vehicles plays a crucial role in the air flow pattern. Unlike WIT and TIT, which are restricted by meteorological conditions, vehicle movement has a persistent and stable effect on the pollution dispersion in the street canyon. The VIT near the road can affect the initial mixing of pollutants, and then change the dispersion process of pollutants. Eskridge and Hunt [27] conducted the first research on the flow structure and turbulence caused by a moving vehicle in the wake area. They derived a theory of the velocity deficit in the vehicle wake in motionless air. Hider [28] extended wake formulation to give the distribution of vehicle velocity in the vertical and cross-wake directions, which further enriched the research results of Eskridge. The results showed that the wake was assumed to be spatially uniform in the area, approximately 20 vehicle heights behind (the far-wake area). The proposal of this theory had attracted many scholars to study and analyze the VIT and its impact on pollutant transport. Qin [29] found that the vehicle-induced air flow was able to affect the range of up to 12 m at the bottom of the street canyon in field observation. Vachon [30] measured the turbulent kinetic energy (TKE) behind the vehicles, and the results showed that the turbulence produced by the moving vehicles significantly increased the TKE on the lower sides of the street canyon, especially on the windward side. Kastner-Klein [31–33] established wind tunnel experiments of vehicle movement in the street canyon. Through the experiments and theoretical analysis, it was found that compared with the impact of environmental wind, the movement of vehicles is an obvious source of turbulence. The results of wind tunnel experiments carried out by Ahmad [34] revealed that the moving vehicles can dramatically lessen the pollution concentration in the street canyon with low wind speed. However, the above methods of field measurement and wind tunnel experiments have the disadvantages of high cost, long measuring time and inability to accurately distinguish VIT from other turbulence sources (WIT and TIT). With the advantages opposite to the above methods, the numerical simulation method has gradually become the main tool for VIT research. Bhautmage [35] used a 3-D CFD relative-velocity approach to study the behavior of airflow around vehicles of different shapes and its effect on the pollution dispersion. Thaker [36] studied the influence of various urban traffic flow patterns on pollution dispersion in an actual asymmetric street canyon by adding the source terms to the turbulence equation. The results showed that free-flow traffic caused larger turbulence in the canyon and a reduction in concentration at pedestrian level. Zhang [37] used CFD method based on a 3-D Euler-Lagrangian model to simulate the air flow in urban street canyons with moving vehicles. The results showed that moving vehicles could pose a forceful effect on wind turbulence in the street canyon, but less impact on average wind field. Nevertheless, there are some limitations in the use of the above numerical simulation methods. For example, the aerodynamic relative speed method can only simulate the situation of one-way traffic, the additional turbulence source term method cannot accurately describe and analyze complex traffic patterns. Apart from the above methods, the dynamic mesh updating technology has also been employed to solve turbulence induced by vehicle movement. In recent years, our research team [38] used dynamic mesh updating technology to simulate the characteristics of moving vehicles in the street canyon and the dispersion of pollutants affected by the moving vehicles. On the basis of this study, Wang [8] studied the characteristics of TKE induced by different speeds of vehicles in the street canyon and the effect of VIT on the dispersion of pollutants. The results demonstrated that the TKE mainly occurs in the vehicle wake and the travelling speed has a crucial impact on the TKE. In vehicle wake, the TKE induced by the vehicle with speed of 15 m/s is about 6.3 times and 1.8 times greater than that induced by the vehicle with the speed of 5 m/s and 10 m/s, respectively. Cai [39] used a dynamic mesh updating method to analyze the TKE induced by a single vehicle under various wind directions and vehicle types. The results showed that the wind direction has an obvious impact on the VIT. The VIT in vehicle wake of the truck is 1.6 times larger than that of the SUV and 2.5 times larger than that of the car under the perpendicular wind conditions.

However, it is not enough to study the turbulence induced by moving vehicles in the street canyon, since moving vehicles are not only the primary factor affecting the flow field at the bottom of the street canyon, but also the major emission source of pollutants. The pollutants emitted by vehicles deteriorate the air quality in the street canyon, compromise the health of pedestrians and the residents in the buildings along the street [40], and also enter the vehicles through the windows or the external circulation system of the vehicle and damage the health of passengers. Dong [41] used the method of large eddy simulation to simulate the exhaust emissions of a light diesel vehicle at idling conditions in the near wake area and analyzed the influence of ambient wind on the flow field in the near wake area. The results showed that vehicular exhaust jet plume dominates the flow field structures and the patterns of pollution dispersion under the conditions of low ambient wind speed. Hu [42] used the numerical aerodynamic relative speed method to simulate the vehicular exhaust jet characteristics of three models and validated the simulation results by wind tunnel experiments. They believed that the dispersion process of exhaust emissions is principally influenced by the wake flow field and is directly related to the velocity field. Ning [43] studied the dispersion characteristics of vehicular exhaust plume at an idling condition by means of field measurement and numerical simulation. They found that the concentration of pollutants drops exponentially in all directions after discharging from the tailpipe, although the initial concentrations are different.

The above different VIT simulation method focused the impact of vehicle movement on the flow field in the street canyon, assuming the vehicle exhaust to be uniform pollution source which is an ideal case

scenario. Moreover, due to the limitation of numerical simulation and experimental methods, the above researches on the vehicle exhaust emissions characteristics were conducted under the idling conditions, lacking the investigation to the exhaust emission of moving vehicles. Different from previous work, this work establish a 3D CFD model which simulates the flow field and pollution dispersion of vehicles in a basic street canyon with the aspect ratio of 1 under the coupling effect of both vehicle movement and exhaust emissions to analyze the real impact of the vehicles on atmospheric environment in the street canyon. This work is the enhancement of previous work and can more accurately predict the pollution environment influenced by vehicles in the street canyons, provides the guidance to drivers to avoid the pollutants emitted by the vehicles in front by keeping the "health distance" calculated by the model.

2. Personal intake fraction (P_IF)

In urban climate science, vehicular population intake fraction (IF) has been adopted to quantify human exposure to air pollutants emitted by vehicles. Vehicular personal intake fraction (P_IF), represents the fraction of total traffic exhausts inhaled by each person on average of a population, which is independent from population size and its density [15]. Hang [44] introduced P_IF into CFD simulations to quantify the average personal exposure of local residents in 2D street canyons.

For a specific pollutant, IF and P_IF are defined as below [45,46].

$$IF = \sum_{i}^{N} \sum_{j}^{M} P_i \times Br_{i,j} \times \Delta t_{i,j} \times Ce_j \Big/ m \tag{1}$$

$$P\_IF = IF \Big/ \sum_{j}^{M} P_i \tag{2}$$

where m is the total emissions over the period considered (kg), N is the number of population groups (children, adults, elders, $N = 3$, $i = 1$ to 3) and M is the number of different micro environments, P_i is the total number of people exposed in the ith population group, $Br_{i,j}$ and $\Delta t_{i,j}$ are the average volumetric breathing rate (m^3/s) and the time spent (s) for individuals in the ith population group in the micro environment j, and Ce_j is the pollutant concentration attributable to traffic emissions in the micro environment j (kg/m^3).

The population data from the National Bureau of Statistics of China [47] was adopted (Table 1). According to Qin [29], time activity patterns for three age groups are classified into four microenvironments: indoors at home (j=1), other indoor locations (j=2), near-vehicle locations (j=3), and other outdoor locations away from vehicles (j=4). In the present study, only the near-vehicle locations (j=3) was considered. The breathing rate and the time activity patterns for individuals in three age groups of $j = 3$ are referred to Allan [48] and Chau [49], as shown in Table 1.

Table 1
Population proportion, breathing rate and time spent in near-vehicle locations for various age group.

Population age subgroups	Population proportion
Children	17.8%
Adults	64.3%
Elderly	17.9%
Population age subgroups	Time percentage for "Near vehicle" (j=3)
Children	5.5%
Adults	7.1%
Elderly	3.2%
Population age subgroups	Breathing rate Br (m^3/day) for "Near vehicle"
Children	14%
Adults	15.5%
Elderly	14.8%

3. Model description

3.1. Geometric model

Street canyons composed of city streets and surrounding buildings are of various forms. According to the aspect ratio of the street canyons (building height/street width H/W), they can be divided into ideal street canyons (H/W = 1), wide street canyons (H/W < 0.7) and deep street canyon (H/W > 1.5) [13,50,51]. Street canyons with viaducts [44,45] and asymmetric street canyons [52,53] have also been extensively studied. Since this paper emphasizes the coupling effect of VIT and exhaust emissions on pollution dispersion, it does not consider the changes of various street canyon types. In this paper, a street canyon near residential areas with narrow lanes was selected as the research object, which is a typical street canyon in cities. The height of residential buildings on both sides of such street canyon is usually low. The traffic on the street is not extremely heavy, but the crowd density is high. Hence, the exposure of pedestrians on such street canyons is a crucial issue.

An ideal one-way traffic street canyon model under the perpendicular wind conditions was established to simulate the above street canyon type. In the model, the width of the street (X-axis direction) is 10 m and equivalent to the height of the buildings (Z-axis direction), that is, the aspect ratio is 1. The length of the street canyon (Y-axis direction) is 80 m. The inlet is 10 m away from the upstream buildings, which is the same as the distance between the outlet and the downstream buildings. The ground is 20 m below the top of the calculation domain.

Sedans and SUVs account for the largest number of vehicles in urban roads. In our previous work, we analyzed the characteristics of TKE generated by various vehicle models, and concluded that the TKE generated by trucks was much higher than that of sedans and SUVs. However, trucks account for a low portion of the vehicles on urban roads. The situation of buses is similar to the trucks. Therefore, only the SUV and the sedan models are considered in this paper. As shown in Fig. 1, the one-way traffic street canyon has two lanes, the width of each lane is 4 m. Each lane has four vehicles, which are two sports utility vehicles (SUV) and two sedans. The dimensions of the SUV model are 4.5 m in length, 1.8 m in width, and 1.5 m in height and the dimensions of the sedan model are 4.2 m in length, 1.8 m in width, and 1.2 m in height. Two tailpipes are symmetrically arranged at the rear of each vehicle. In the actual road, the wheel rotation always brings dust, but its impact on TKE and exhaust emission is relatively small. Hence, the impact of wheels is ignored, the vehicles are directly placed on the plane at Z = 0.4 m. Four vehicle speeds (namely 5 m/s, 10 m/s, 15 m/s, 20 m/s) are selected to study the influence of vehicle speed on the combined effect of both vehicle movement and exhaust emission on pollution dispersion in the street canyon.

3.2. Mathematical model

The renormalization group (RNG) k-ε model has been widely applied to simulate complex airflow in buildings and urban areas [6]. Chan [54] used a series of k-ε models to simulate the flow field in the two-dimensional street canyon. They found that the simulation results of RNG k-ε model were in agreement with the results of the wind tunnel experiment. Thereby, the CFD software FLUENT 19.0 with the RNG k-ε model was utilized to simulate the VIT and exhaust emission. The mathematical model adopted at present is the same as our previous work [39]. The comprehensive mathematical model including the Mass equation, Navier-Stokes equations, component transport equation, and RNG k-ε equations can be written as follows:

Mass equation:

$$\frac{\partial U_i}{\partial x_i} = 0 \tag{3}$$

Conservation of momentum equation:

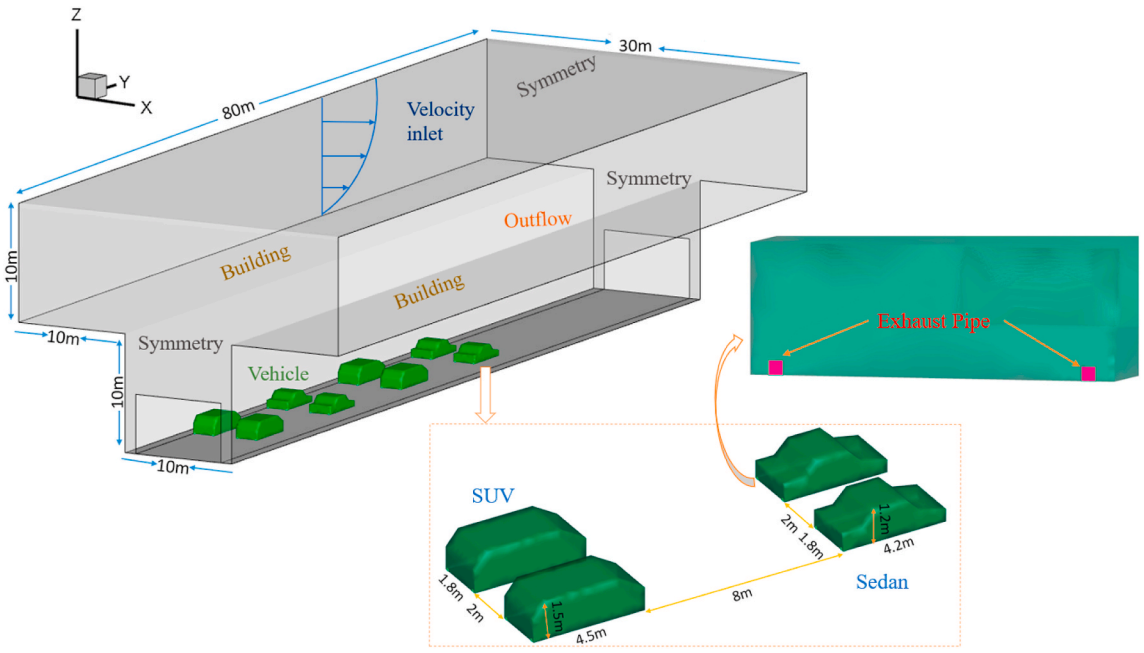

Fig. 1. Geometric model.

$$\frac{\partial U_i}{\partial t}+U_i\frac{\partial U_j}{\partial x_j}=-\frac{1}{\rho}\frac{\partial p}{\partial x_i}+\frac{\partial}{\partial x_j}\left(\nu\frac{\partial U_i}{\partial x_j}+\frac{\partial U_j}{\partial x_i}-\overline{u_i'u_j'}\right)+\left(\frac{\rho-\rho_0}{\rho_0}\right)g_i \tag{4}$$

where $\overline{u_i'u_j'}$ is the Reynolds stress term, $\overline{u_i'u_j'}=\nu_t\frac{\partial U_i}{\partial x_j}+\frac{\partial U_j}{\partial x_i}-\frac{2}{3}\delta_{ij}k$.

Component transport equation:

$$\frac{\partial C_i}{\partial t}+U_j\frac{\partial C_i}{\partial x_j}=\frac{1}{\rho}\frac{\partial}{\partial x_j}\left[\left(D_i+\frac{\mu_t}{Sc_t}\right)\frac{\partial C_i}{\partial x_j}\right] \tag{5}$$

Turbulent kinetic energy equation k:

$$\frac{\partial k}{\partial t}+U_j\frac{\partial k}{\partial x_j}=\frac{\partial}{\partial x_j}\left[\left(\nu+\frac{\nu_t}{\sigma_k}\right)\frac{\partial k}{\partial x_j}\right]+\mathrm{G}-\varepsilon \tag{6}$$

where ν_t is the turbulent viscosity coefficient, $\nu_t=C_\mu\frac{k^2}{\varepsilon}$.

Dissipation rate of turbulent kinetic energy ε:

$$\frac{\partial \varepsilon}{\partial t}+U_i\frac{\partial \varepsilon}{\partial x_i}=\frac{\partial}{\partial x_j}\left[\left(\nu+\frac{\nu_t}{\sigma_\varepsilon}\right)\frac{\partial \varepsilon}{\partial x_j}\right]+C_{1\varepsilon}\frac{\varepsilon}{k}\mathrm{G}-\left[C_{2\varepsilon}+\frac{C_\mu\rho\eta^3\left(1-\frac{\eta}{\eta_0}\right)}{1+\beta\eta^3}\right]\frac{\varepsilon^2}{k} \tag{7}$$

The constant value used in (1)-(4), respectively, $C_\mu=0.09$ $C_{1\varepsilon}=1.42$, $C_{2\varepsilon}=1.92$, $\sigma_k=1.0$, $\sigma_\varepsilon=1.3$ $\eta_0=4.38$, $\beta=0.0012$, $\eta=0.5\left(\frac{k}{\varepsilon}\right)\left(\frac{G}{\nu_t}\right)$ [55].

3.3. The dynamic mesh updating method

When the car moves in the street canyon, the mesh around the vehicle will be deformed accordingly. Therefore, the deformed mesh needs to be adjusted with time to make it satisfy the requirements of calculation. The update of mesh is automatically processed by FLUENT solver [56,57]. Compared with the static mesh model, the dynamic mesh updating method are capable of solving the problem that the mesh shape changes with time because of the moving objects' boundary change. Due to its strong applicability, the unstructured mesh is the basis for dynamic mesh technology. Therefore, the unstructured mesh is set in the region of vehicle movement. The dynamic mesh updating method utilized in this paper is the same as our previous work [8,39], which shows the specific information in detail. There are two parameters, the general scalar, ϕ, and the arbitrary control volume, V in the dynamic mesh updating method, which should be carefully addressed as follows [58]:

$$\frac{d}{dt}\int_V\rho\varphi dV+\int_V\rho\varphi(\vec{u}-\vec{u_g})d\vec{A}=\int_{\partial V}\Gamma\nabla\varphi\cdot d\vec{A}+\int_V S_\varphi \mathrm{dV} \tag{8}$$

$$\frac{d}{dt}\int_V\rho\varphi dV=\frac{(\rho\varphi dV)^{n+1}-(\rho\varphi dV)^n}{\Delta t} \tag{9}$$

$$V^{n+1}=V^n+\frac{dV}{dt}\Delta t \tag{10}$$

$$\frac{dV}{dt}=\int_{\partial V}\overrightarrow{U_g}\cdot d\vec{A}=\sum\overrightarrow{U_{g\,j}}\cdot\vec{A_j} \tag{11}$$

$$\overrightarrow{U_{gj}}\cdot\vec{A_j}=\frac{\delta V_j}{\Delta t} \tag{12}$$

In these equations shown above, S_φ is the source term of the scalar φ, n and n+1 are the current and next time level, respectively, $\vec{A_j}$ is the area vector in the j area, δV_j is the volume swept by the control volume face j at each time step Δt.

In FLUENT 19.0, we used user-defined functions (UDF) to describe the effect of transient movement of several vehicles in the street canyons. In the present simulation, the time step size is set to vary from 0.0005 s to 0.002 s according to the different vehicle speeds to avoid the grid from increasing to a tremendous skew rate. The maximum iteration step is set to 100 to achieve a converged calculation result in each iteration step. In addition, the finite volume method and the fully implicit scheme are adopted to perform spatial and temporal discretization on the Navier-Stokes equations of the flow field.

3.4. Boundary conditions

The boundary conditions set in the present simulation are also presented in Fig. 1. The inlet was set as the velocity-inlet. At the outlet boundary, an outflow condition was imposed, which means a zero

normal first derivative of all quantities. The surface of the ground and buildings as well as the vehicles were set as non-slip walls. The exhaust tailpipe is set as the velocity-inlet. In order to simplify the analysis, carbon monoxide (CO) was selected as a vehicular pollutant to study the dynamic dispersion characteristics of exhaust pollution. The concentration of CO at the tailpipe exit is 10 ppm. The exit velocity at the tailpipe is 5.5 m/s. The exhaust gas temperature was set to 380 K. The ambient wind profile in this paper is expressed by the exponential law [59]. The exponential velocity curve of the velocity inlet and the corresponding turbulent kinetic energy k and dissipation rate ε are defined as follows through user-defined functions (UDF):

$$U_Z = U_{ref}\left(\frac{z-10}{z_{ref}}\right)^a \tag{13}$$

$$k = \frac{U_*}{\sqrt{c_\mu}} \tag{14}$$

$$\varepsilon = \frac{{U_*}^3}{Kz} \tag{15}$$

k is the von Karman constant (0.4) $a = 0.22$, $c_\mu = 0.09$ [60]. Since this paper focuses on vehicle movement and exhaust emissions, the impact of the other two mechanisms should be minimized. The reference wind speed U_{ref} is the ambient wind velocity at the reference height z_{ref} (set to 10 m), which is set to be 2 m/s. It meets the actual situation and the simulation requirements.

3.5. Meshing skills and computational procedure

Since the size of the tailpipes are very tiny compared to the entire calculation domain, the mesh around the tailpipes were set to the similar small size. In order not to make the ratio between the adjacent grids too large, an unstructured grid was used. However, the unstructured grid has the disadvantages of slow generation speed and poor mesh quality. On the contrary, the structured mesh has the advantages of fast generation speed, high quality and simple data structure. Therefore, in order to improve the overall mesh quality, two mesh patterns were adopted in this model. The unstructured grid was set around the vehicle movement region, and the structural mesh was set in the rest of the domain. The mesh near the wall surface were densified, the y+ of the first-layer mesh met the calculation requirements. The mesh at the bottom of the street canyon, especially the region around the vehicle tailpipes, were also densified to improve the calculation accuracy. The minimum mesh size near tailpipes and the boundary layer was 0.01. The mesh of the region over and distance away from the street canyon were selected to be relatively sparse, for reducing the calculation time. Fig. 2 shows the schematic diagram of the mesh demarcation.

The Green-Gauss node based and second-order upwind scheme were selected for the discretization of convection and diffusion terms. The SIMPLE algorithm was adopted to solve the motion of vehicles. The convergence criteria was that the maximum residuals of the species, mass, and momentum were less than 1×10^{-5}; and those for energy equation were less than 1×10^{-8}.

To verify the grid independence, three grid numbers of 1,759,662, 2,523,791, and 3,604,223 were selected in this study and calculated under the same working conditions (U_{ref} was 2 m/s, the vehicles were under idling condition), and the results on the street centerline along the X-axis are plotted in Fig. 3. The X-velocity and the TKE of this line under the three mesh systems were selected for comparison. It is shown in Fig. 3 that the maximum error of the X-velocity and the TKE is less than 10%. The maximum error occurs when the grid number is 1,759,662. It is approximately the same as the test results for grid numbers of 2,523,791 and 3,604,223. That means that further increases in the number of grids will not cause significant deviations in the major computational parameters, hence the accuracy of numerical solution and the independence of grid are validated. Thus, grid number 2,523,791 was chosen as the basic grid system in this study.

3.6. Model validation

3.6.1. For flow field

The data used to evaluate the CFD model in this study were obtained from Kastner-Klein et al. [31]. The wind tunnel experiment was performed at the Institute of Hydromechanics, University of Karlsruhe. An isolated street canyon with H/W = 1 and L/H = 10 was mounted in a neutrally stratified wind tunnel. The mean velocity components and turbulence data in five given cross-sections along the height direction were obtained by laser Doppler velocimetry and hot-wire anemometry. The two-lane traffic in an urban street was simulated by rectangular plates mounted on two moving belts stretched along the canyon. In order to compare with the wind tunnel data, the case with vehicles moving at velocity V = 5.0 m/s, $u_{ref} = 7$ m/s, and the vehicle distance of 0.20 m was modelled, with the two-lane vehicles moving in the same direction. The comparison between the wind tunnel data and the numerical simulations about mean horizontal (u), vertical velocity (w) and TKE profile is present in Fig. 4, where TKE was defined and was calculated based on the three components of measured root-mean-square velocity fluctuations:$\kappa = \frac{1}{2}(\overline{(u')^2} + \overline{(v')^2} + \overline{(w')^2})$. The horizontal (u) and vertical velocity (w) magnitudes were divided by u_{ref} (u_{ref} is the wind velocity at the reference height) to determine the normalized velocity component. The normalized TKE was defined as TKE divided by the square of u_{ref}. To evaluate the prediction accuracy of the present simulation results, we selected the data of the windward position (X/H = 0.375 plane) for comparison.

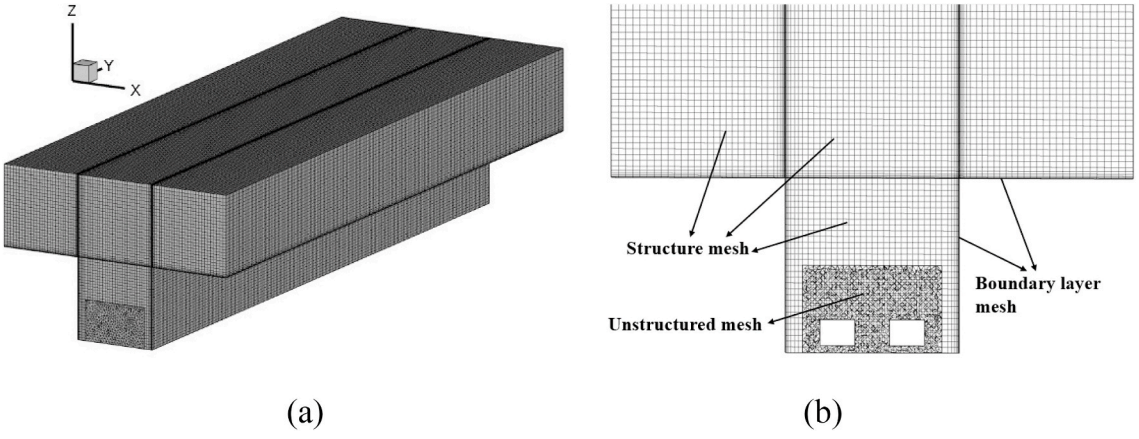

Fig. 2. Schematic diagram of the mesh: (a) Mesh of the calculation domain; and (b) Mesh of the vehicle's cross section.

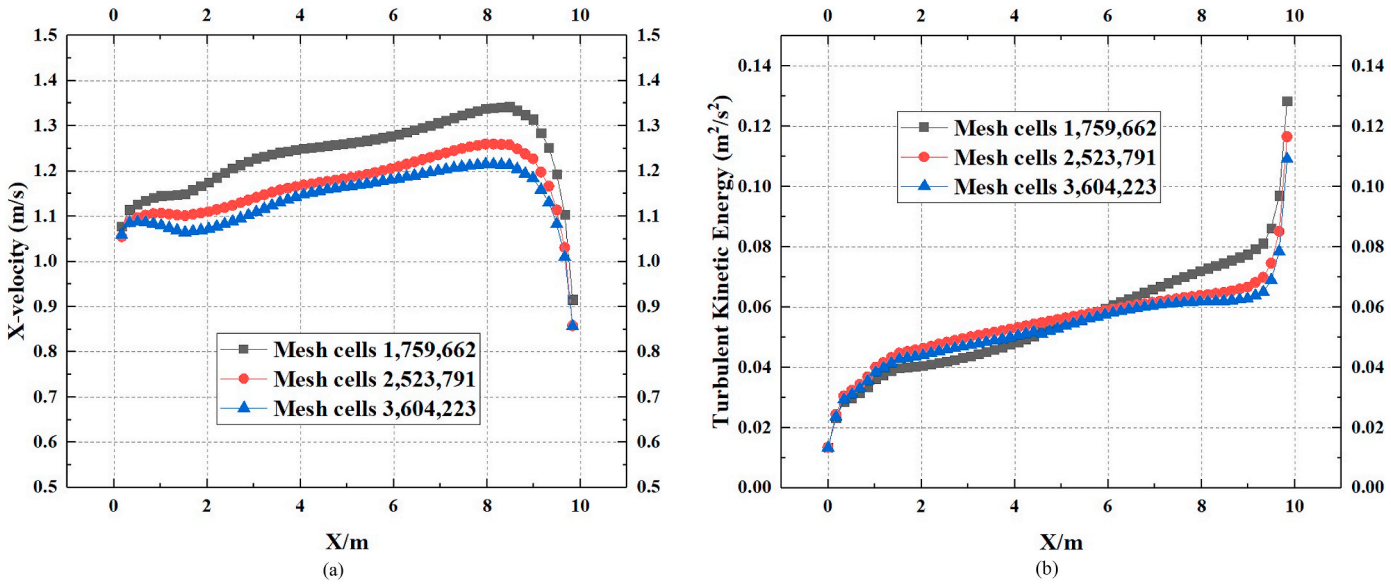

Fig. 3. Grid independence test results: (a) X-velocity; and (b) turbulent kinetic energy.

As can be seen from Fig. 4, the present simulation results are basically in good agreement with the wind tunnel data, but the three selected parameters are slightly underestimated. A reasonable explanation is that, unlike the wind tunnel experiment that uses rectangular plates to simulate the traffic flow, the vehicle models used in the numerical simulation are more realistic and streamlined. As a result, the relative motion intensity between the windward surface of the vehicle and the surrounding air deceases, which affects the flow structure in street canyon. Thus, a slight difference in the magnitude of velocity component and TKE is acceptable.

3.6.2. For vehicle exhaust jet

To verify the reliability of the present CFD numerical model for vehicle exhaust jet simulation, the model validation in this paper is compared with Ning's [4] vehicle exhaust emission measurement experiments. Ning's experiment measured the exhaust emissions of the car at the idling condition in a semi-closed space considering the vehicles waiting for passengers or stopping at a red light. In order to reduce the impact of ambient wind and solar radiation on the exhaust diffusion, the experiment was conducted under weak ambient wind and in the evening with stable weather conditions, and the temperature and relative humidity were 20–22 °C and 50–60% respectively. They measured a variety of exhaust products, and we chose the CO_2 for comparison. Additionally, they carried out numerical simulation with the same conditions as the actual measurement. The diameter of the tailpipe was 0.03 m, and the height above the ground was 0.3 m. The exhaust speed was 4.8 m/s, the temperature of exhaust gas at the tailpipe exit was set to be 380 K. Fig. 5 shows the dispersion characteristics of CO_2 along the centerline of the vehicle tailpipe. Generally speaking, the simulated profiles are in good agreement with the experimental data. The simulated values of CO2 concentration in the present study decrease faster than the experimental values between 0 and 3 m. When the distance is larger than 3 m, the simulated plumes of our work are comparable to those of Ning, and both simulation results are slightly higher than the experimentally determined plumes. The error between these two results was caused by the facts that the experimental measurement was not undertaken in an entirely windless environment, and the low wind speed accelerated the diffusion of CO_2.

4. Results and discussion

4.1. Characteristics of exhaust pollution dispersion in the process of vehicle movement under various car arrangements

The vehicles on the street were arranged in manifold ways, which had a crucial impact on the flow field and the distribution of exhaust pollution at the bottom of the street. This subsection analyzes the dispersion of exhaust pollution under two common vehicle arrangement modes, namely the in-line arrangement and the staggered arrangement.

4.1.1. Vehicles being arranged in line

Fig. 6 shows the distribution of vehicles exhaust CO at the tailpipe height of Z = 0.44 m at different moments when the vehicles are travelling in line with the speed of 5 m/s. The vehicles are in the idle state when t = 0. Affected by the ambient crosswind in the bottom of the street canyon, the exhaust emitted by the vehicles is blown to the leeward side, and the exhaust jet plume is relatively short, about 4 m in the Y-axis direction. When the vehicles start to move, according to aerodynamic relative motion theory, the effect of the vehicles moving at 5 m/s on the surrounding air flow is equal to the air flowing to the stationary vehicle with the same speed in the opposite direction. Compared to the idle state, the vehicles' exhaust jet plume becomes longer. The crosswind velocity at the bottom of the street is very low relative to the vehicle speed, so the exhaust jet plume becomes to parallel to the moving direction of the vehicle. This also proves that VIT plays a dominant role in the flow field at the bottom of the street canyon. At t = 0, the pollutants emitted by the vehicles are concentrated near the tailpipe. With the moving time increasing, the exhaust pollutants gradually diffuse in the vehicle wake, and its distribution become more even in the street canyon.

4.1.2. Vehicles being arranged staggered

The CO contours at tailpipe height (Z = 0.44 m) at different moments when the vehicles travelling staggered with the speed of 5 m/s are shown in Fig. 7. Similarly, the vehicle exhaust is blown to the leeward side at the idle state. When the vehicle starts to move, the exhaust jet plume begins to parallel to the direction of vehicle movement. Due to the location of the car, vehicles driving in the leeward side lane are more susceptible to the impact of the exhaust pollution from the vehicles in front. Especially when the vehicle just starts or is under the condition of high ambient wind velocity and low vehicle speed, the exhaust emitted

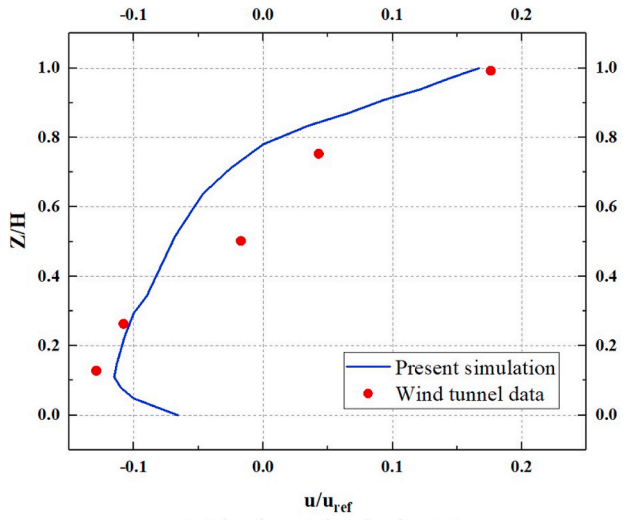

(a) horizontal velocity (u)

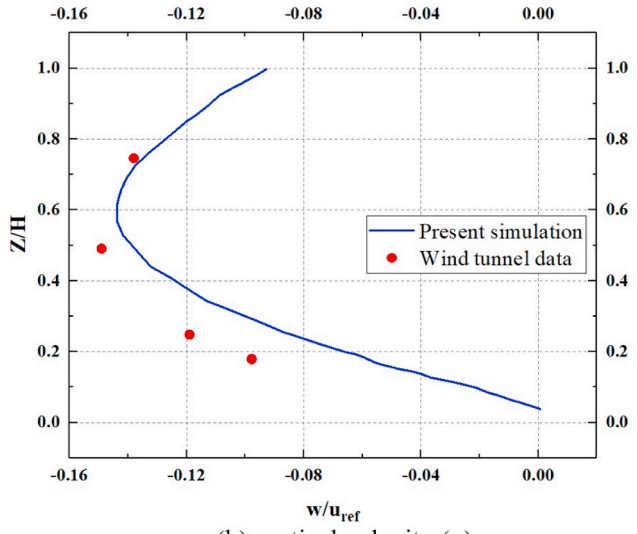

(b) vertical velocity (u)

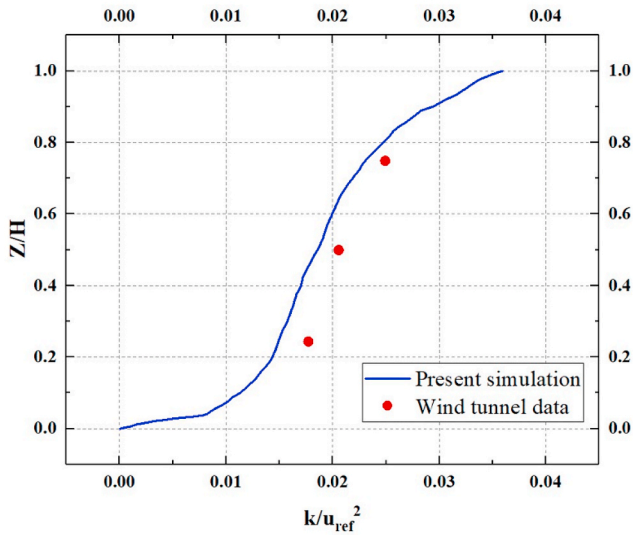

(c) the normalized TKE

Fig. 4. Comparison between the wind tunnel experiments data and the numerical simulation results: (a) horizontal velocity profile; (b) vertical velocity profile; and (c) the TKE profile.

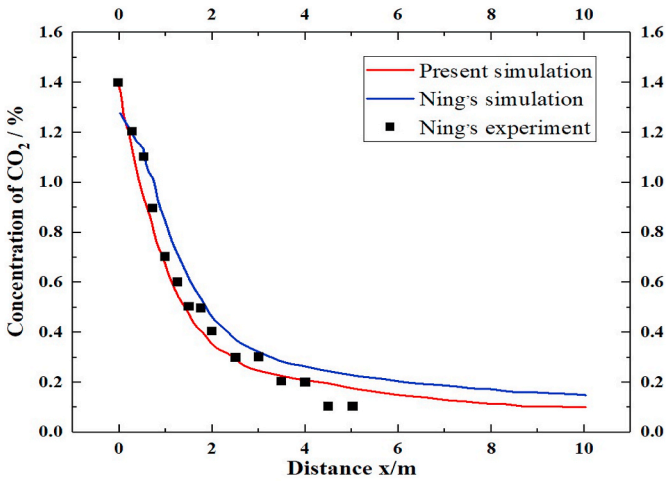

Fig. 5. Comparison of CO_2 between the simulated result and experimental data.

from the vehicle in front may enter the interior of the vehicle behind directly through the window.

It is clear that the distribution of CO for the vehicles in staggered arrangement is more uniform than that of the vehicles in-line arrangement. This is because that the staggered vehicles disturb the flow field at the bottom of the street canyon, enhance the turbulence, and accelerate the mixing of vehicles exhaust and clean air.

4.2. *Effect of different factors on exhaust pollution dispersion*

4.2.1. *Vehicle speed*

In this subsection, four different speeds are set at: 5 m/s,10 m/s, 15 m/s and 20 m/s, to explore the influence of vehicle speed on the characteristics of VIT and the diffusion of vehicle exhaust pollutants. Fig. 8 shows the TKE contours of the vehicle with the speed of 5 m/s, 10 m/s, 15 m/s and 20 m/s respectively in the Z = 1 plane at t = 1s. As shown in Fig. 8, the faster the speed of the vehicle, the higher TKE induced by the vehicle, and the larger the range of the high TKE in vehicle wake. The increase in turbulence intensity and the range of VIT accelerates the diffusion of exhaust pollution in the street canyon, thus making the exhaust pollution evenly distributed.

The mass fraction of CO at the leeward sidewalk (X = 1.5 m) with breathing height of Z = 1.5 m in the direction of vehicle movement is shown in Fig. 9. It can be seen that when the vehicles are moving at 5 m/s, the pollutants accumulate in several areas. The concentration in these areas is much higher compared to that in the rest areas. This phenomenon is alleviated when the vehicle speed is increased to be 10 m/s and 15 m/s. With the vehicle speed increasing to 20 m/s, the change of pollution concentration is relatively smooth. It can be concluded that, within the same time period of the movement, the faster the vehicle speed, the more uniform the pollution distribution in the street canyon. This is because the high TKE induced by fast vehicles accelerates the mixing process between the exhaust pollutants and the surrounding air. In addition, the tailpipe of a high-speed vehicle has a larger displacement in the same time period, the vehicles emit the same amount of exhaust pollutants over a longer distance. Consequently, vehicle speed determines the size and range of VIT, thus has a crucial impact on the dispersion of vehicle exhaust pollutants.

4.2.2. *Ambient wind velocity*

In this subsection, we set different ambient wind velocities at: 1 m/s, 2 m/s, 4 m/s and 8 m/s, to explore the effect of ambient wind velocities on vehicle exhaust emissions. Fig. 10 shows the distribution of vehicles exhaust CO at the tailpipe height (Z = 0.44 m) with the speed of 15 m/s

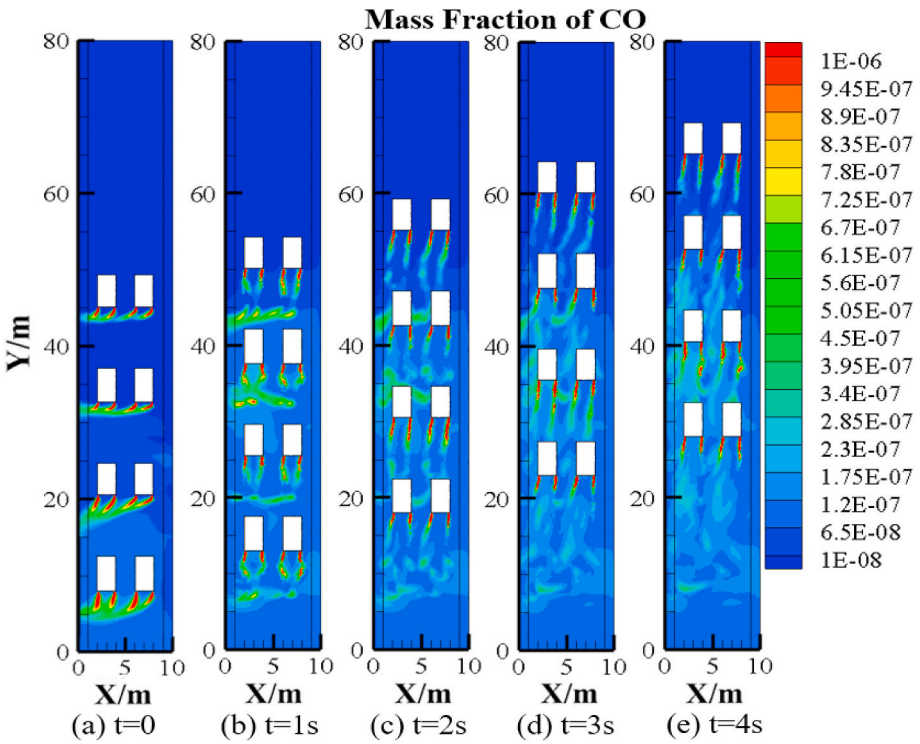

Fig. 6. Contours of CO when the vehicles are travelling in line at different times in the Z = 0.44 m plane.

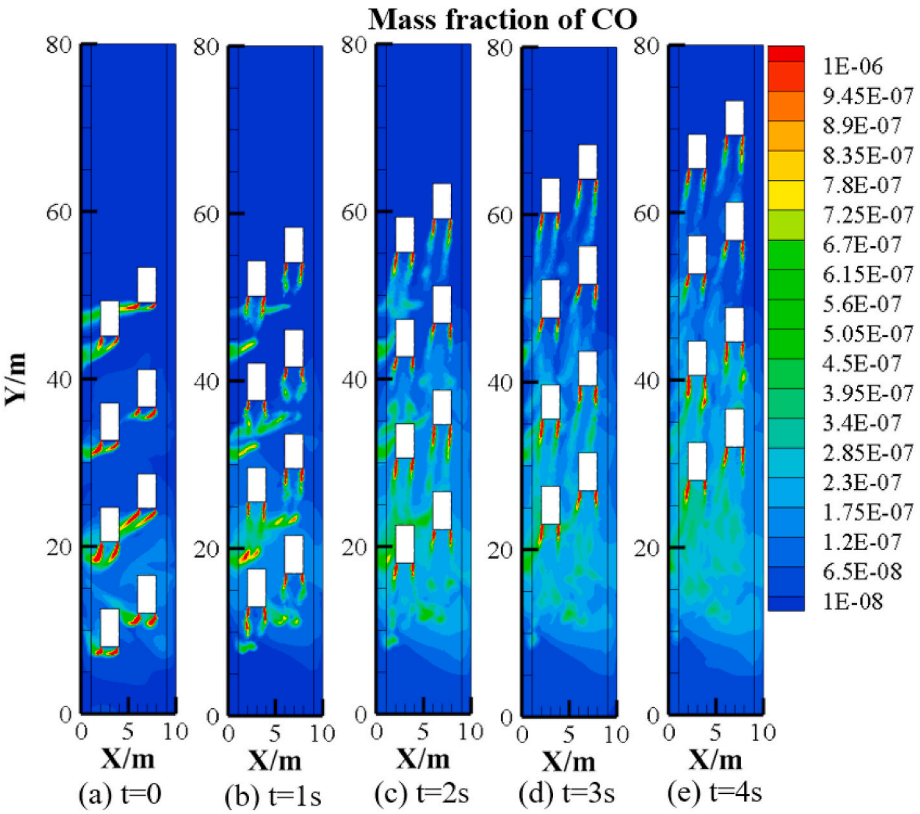

Fig. 7. Contours of CO when the vehicles are travelling staggered at different times in the Z = 0.44 m plane.

under different ambient wind velocity. It can be seen from Fig. 8 that the ambient wind has a crucial influence on the vehicular exhaust jet plume. When the ambient wind speed is 1 m/s, the vehicular exhaust jet plume is inclined to the leeward side, and its length is approximately 4 m in Y-axis direction. The jet length becomes shorter, with the ambient wind speed increasing. The vehicle exhaust can hardly jet in the Y-axis direction and is blown directly to the leeward side when the ambient wind velocity is 8 m/s.

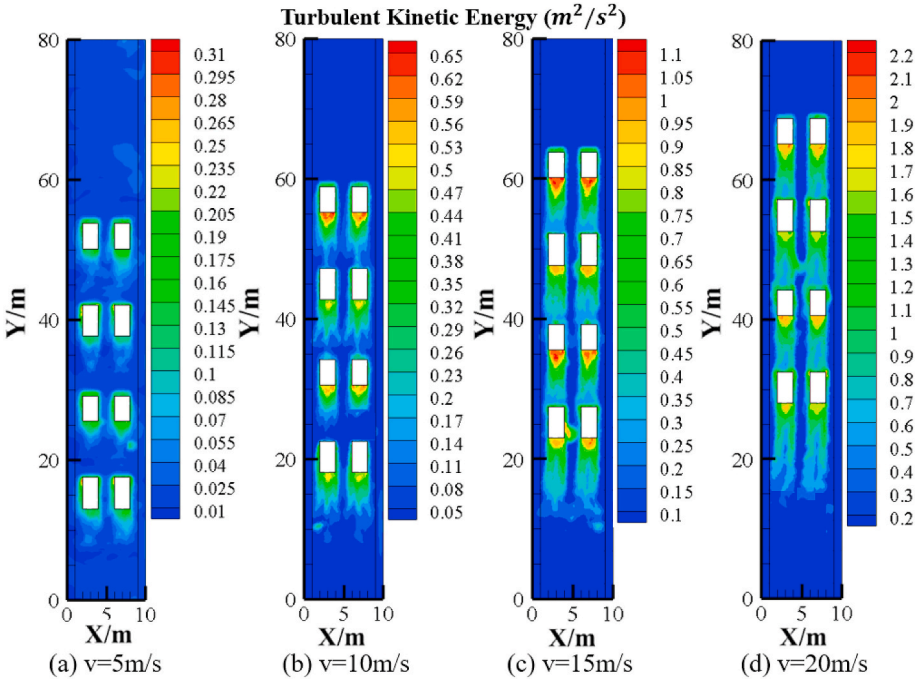

Fig. 8. Contours of TKE when the vehicle drives with different speeds in the Z = 1 m plane at t = 1 s.

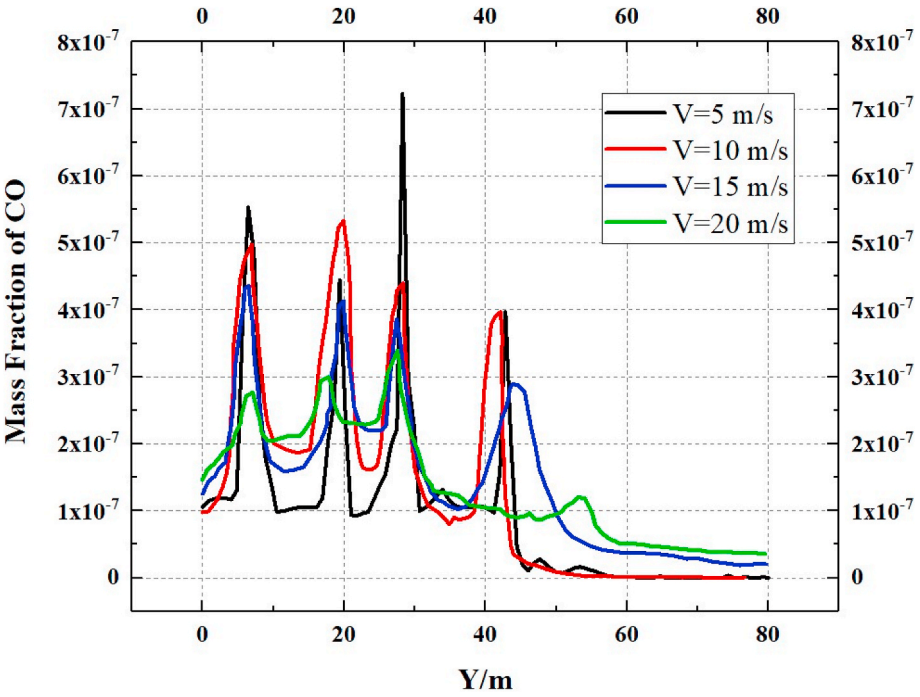

Fig. 9. CO concentration profiles at the height of Z = 1.5 m in the leeward sidewalk (X = 1.5 m).

When the vehicles start to move, the exhaust jet plume flows toward the moving direction of the vehicle due to the high speed of the vehicle relative to the ambient wind at the bottom of the street canyon, and the jet length also increases compared to the case when the vehicle is at the idle state. With the increase of the ambient wind speed, the exhaust pollution accumulated around the tailpipe of the vehicles at the idle state reduces, and the pollution concentration of the entire street canyon decreases.

4.2.3. Personal intake fraction (P_IF)

Fig. 11 shows the personal intake fraction (P_IF) on windward and leeward sidewalks under the influence of the above two factors at t = 1s. In general, affected by the crosswind at the bottom of the street canyon, the pollution concentration on the leeward side is significantly higher than that on the windward side. The impact of the change in ambient wind velocity on P_IF is very interesting. On the windward side, the P_IF decreases with the increase of ambient wind velocity; while on the leeward side, when the ambient wind velocity increases, the P_IF increases first and then decreases. This is because when the ambient wind

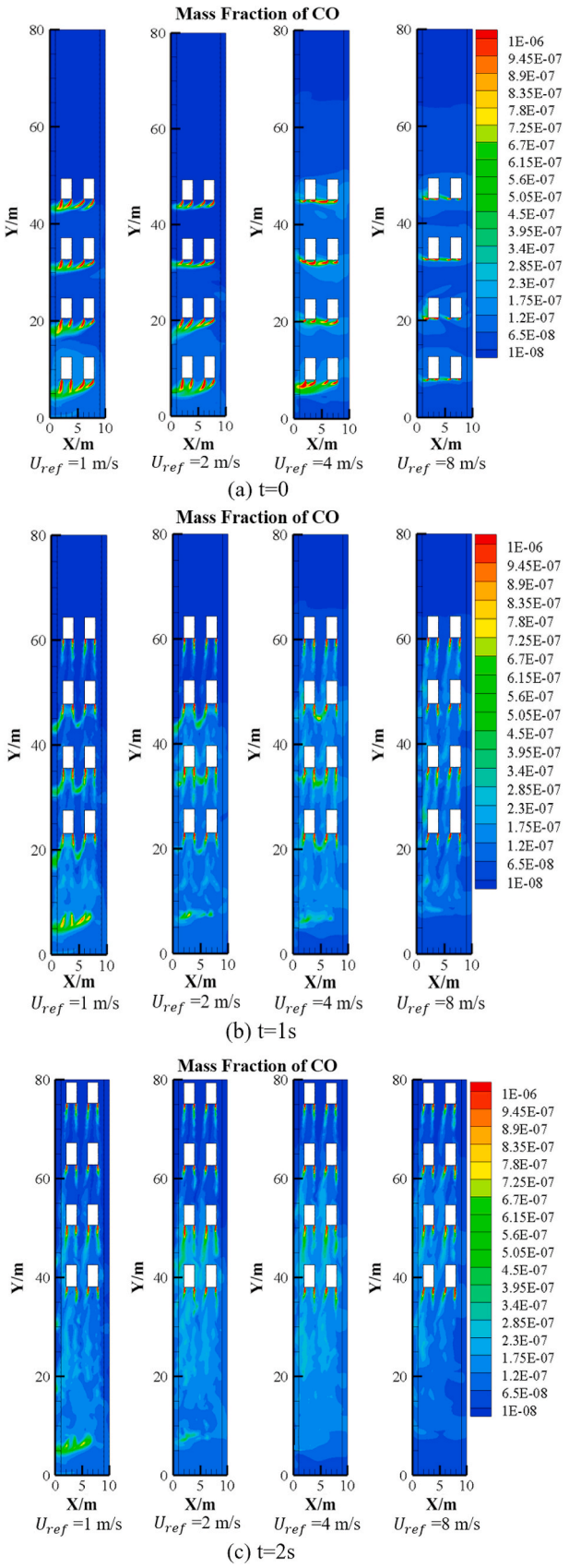

Fig. 10. Contours of CO at different time points in the Z = 0.44 m plane under four ambient wind velocities: (a) t = 0; (b)t = 1s; and (c) t = 2 s.

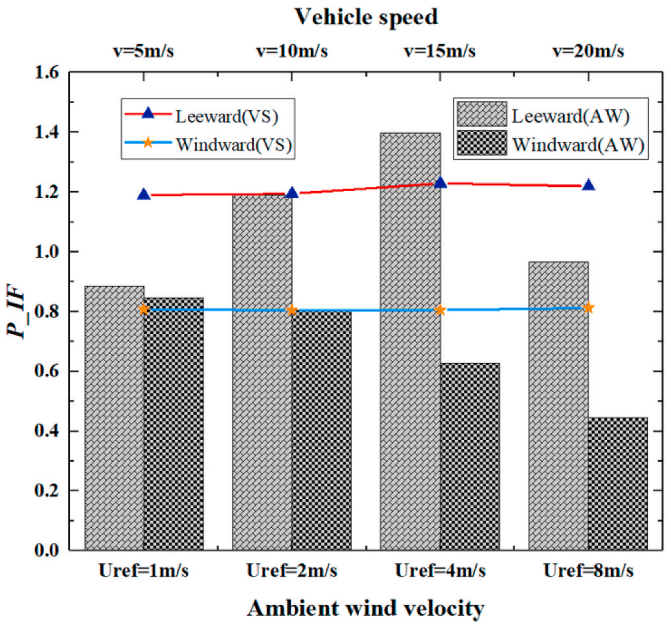

Fig. 11. The personal intake fraction (P_IF) in windward sidewalk (X = 8.5–10 m) and leeward sidewalk (X = 0–1.5 m).

velocity increases, the turbulence intensity in the street canyon increases, which accelerates the transport of pollution from the windward side to the leeward side, leading to the P_IF increase on the leeward side first. As the ambient wind velocity continues to increase, the airflow exchange between the interior and the upper part of the street canyon continues to increase, and the vehicle exhaust pollutants from the leeward side are carried out of the street canyon. Therefore, the P_IF on the leeward subsequently decreases, while the P_IF on the windward side always decreases. However, when the ambient wind velocity is 2 m/s, P_IF is unaffected by the vehicle speed, and the fluctuation range is about 5% on both windward and leeward side. It can be explained that, different from previous studies which simulated the continuous traffic flow, the present model simulates the exhaust pollution dispersion of specific vehicles moving in a limited street canyon for a short period of time. High-speed moving vehicles can enhance the mixing of the vehicle exhaust with the clean air, making the pollution evenly distributed in the street canyon. However, this phenomenon only happens at the bottom of the street canyon, and the influence of VIT effect on the air exchange in the upper part the street canyon is not obvious. Therefore, within the same time period, the P_IF varies little with vehicle speed, which is mainly affected by the ambient wind velocity.

4.3. The investigation on the dispersion range of vehicle exhaust pollutants and VIT in the wake of vehicles

The above study simulated the vehicles from the idle state to moving in a short time period, focusing on the VIT's effect, the initial mixing, diffusion process of exhaust pollutants and surrounding air, when the dispersion of TKE and exhaust pollutants in the vehicles wake has not reached a stable state within a short period of time during vehicle's movement. For instance, before the vehicles with the speed of 20 m/s reach the end of the street canyon, the range of the VIT in vehicles wake increases. In order to explore the time period for dispersion of VIT and the exhaust pollutants in the wake of the vehicle with constant steady speed, in this subsection, a 200 m long street canyon model was constructed. In this model, the distance of vehicle moving is extended to 33 m to investigate the range of dispersion of exhaust emissions and the VIT in the wake of the vehicles at the stable state. Two rows of cars were simulated. The first row is sedans and the second row is SUVs for researching case with different types of vehicles. The rest of the settings

of the model are the same as those of the first model.

Fig. 12 shows the TKE contours along the center of the vehicles with the speed of 5 m/s at different time points. It can be seen that the range of the VIT in the vehicles' wake continuously increases from 0 s to 6 s, and reaches the stable state when t = 7 s. The range of the VIT is about 15 m behind the rear of the vehicle in the direction of movement for sedans, and 18 m for the SUVs. In the upward direction vertical to the ground, the range of the VIT decreases along the direction of the exhaust jet, from the roof height at the beginning to about 0.8 m at the end. The same results are also drawn in the case when v = 10 m/s. The time period for the vehicle accelerating from the idling state to the steady moving state is about 7 s. Moreover, it can be seen from this case that the range of the VIT in the vehicle's wake generated by SUVs is larger than that generated by sedans. The VIT range of SUVs is about 38 m in Y-axis direction, and that of sedans is about 30 m. The possible reason is that the cross-sectional area of the SUV is greater than that of the sedan, and the sedan is relatively more streamlined.

Fig. 13 shows the CO contours along the tailpipe center of two types of vehicles with v = 5 m/s at a stable state. As shown in Fig. 13, the concentration of exhaust pollution of two vehicle models drops from about 8 m in the Y-axis direction behind the tailpipe to less than 1% of the concentration of exhaust emission. In the direction vertical to the ground, because the temperature of the exhaust is higher than that of the surrounding air, it diffuses upward under the influence of thermal buoyancy, but it does not exceed the height of the car roof. This is because the speed of the car relative to the air above the car roof is much higher than the speed of the exhaust gas floating, thus the exhaust gas is blown downstream when it diffuses to the height of the car roof. Interestingly, by comparing the range of exhaust pollutants at different speeds, we find that there is not apparent correlation between the vehicle speed and the range. We believe that the range of 8 m behind the vehicle is directly affected by its exhaust emissions. If the distance between two vehicles is less than 8 m, the exhaust pollutants emitted by the car in front will enter the interior of the following car through its the window or the external circulation system, compromising the air quality in the following car and harming the health of the people inside the car. Therefore, when driving a car, the driver should not only follow a safe physical distance but also maintain a "heathy distance" taking into account the air quality inside the car.

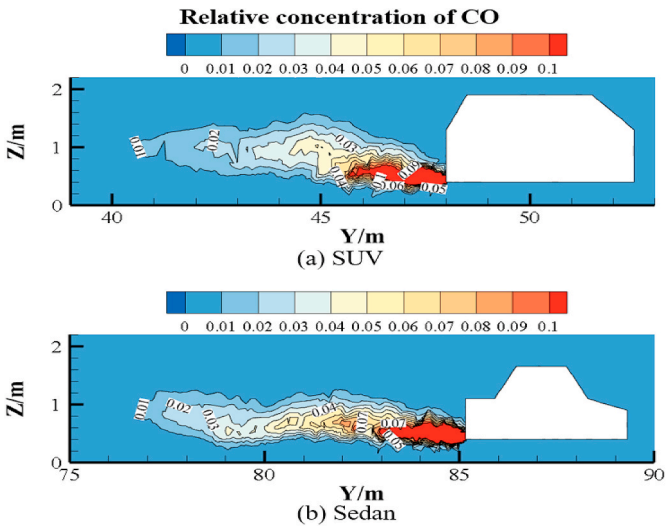

Fig. 13. Distribution of CO relative concentration at X = 17.06 m for different vehicle model: (a) SUV; and (b) Sedan.

Generally, the "3-s interval" is used to determine the safe distance from the vehicle in front, that is, to control the distance of driving for 3 s at the current speed. For example, when the vehicle is travelling at a speed of 5 m/s, the required safe distance is 15 m; at a speed of 10 m/s, it is 30 m. These are similar to the range of high TKE in the wake of vehicle obtained by our previous simulation results. That means that when the vehicles travel on the road at a "safe distance" to form a stable traffic flow, the turbulence induced by vehicles' movement can be regarded as the source of a continuous turbulence. Compared with the range of VIT, the range of dispersion of exhaust emission is relatively small and the concentration of pollution decreases rapidly. Therefore, it is difficult to form a stable and uniform pollution source from the limited vehicle's exhaust emissions. However, the continuous traffic flow continuously produces exhaust pollutants influenced by the VIT effect. In the

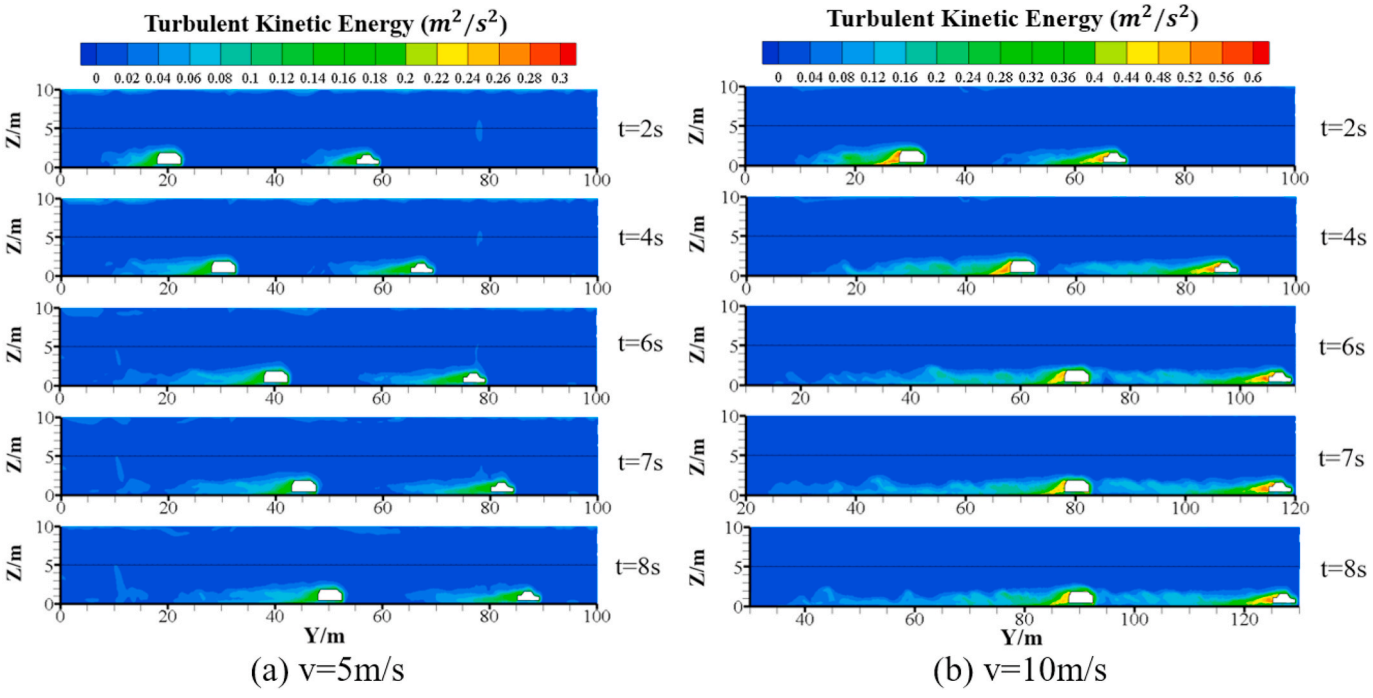

Fig. 12. TKE contours in the X = 17.06 m plane at different time points: (a) v = 5 m/s; and (b) v = 10 m/s.

meantime, the ambient wind can carry part of pollutants out of the street canyon, thereby forming the dynamic changes of vehicles' exhaust pollutants at the bottom of the street canyon, which will be studied in the next stage.

5. Discussion

In this paper, the dynamic mesh updating technology is employed to simulate the exhaust emission process of moving vehicles, and analyze the effects of vehicles arrangement and other factors including vehicle speed and ambient wind velocity on the pollution dispersion in the street canyon. This validated novel simulation technology provides a new method to study vehicle exhaust pollution in the future.

Nevertheless, there are some limitations in current work, which will be addressed by our further work in next stage. Firstly, we choose CO to study the characteristics of vehicular exhaust pollution dispersion, without considering the main components of vehicular exhaust such as particulate matter and NOx. In addition, the mass fraction of CO emitted by the vehicles in all cases was set to be the same, without considering the changes of exhaust emission due to the changes in the vehicle's operating state. Secondly, a narrow street canyon of one-way traffic near urban residential areas was selected for modeling, which is different from the wide street canyons of arterial roads with two-way traffic. The interaction between vehicles travelling in the opposite directions will be studied in the next stage. Moreover, in the next stage we will investigate more complicated urban streets including street canyons with viaducts and asymmetric street canyon.

This paper explores the condition of the general assumptions that the turbulence induced by vehicle movement is continuous turbulence source and the vehicle exhaust emissions is uniform pollution source in the street canyon. The research indicates that VIT can be regarded as a continuous turbulence source when the vehicles travel at a "safe distance" on the road to form a stable traffic flow. However, the dispersion of vehicle exhaust emissions in the street canyon is affected by the thermal buoyancy, gravity deposition, ambient wind, and the VIT effect. It is a long-term process to achieve dynamic equilibrium of the deposition and dissipation of exhaust pollutants in the street canyon. If the current method is used to simulate the movement and exhaust process of a large number of vehicles over a long period of time, a tremendous calculation domain needs to be established. Additionally, since the size of the tailpipe is extremely tiny compared to the physical size of adjacent components of the vehicles, the cross-scale simulation is required, and the calculation times required would be enormous. Therefore, in the next step, we will explore new methods to reduce the amount of calculation, for instance using periodic boundary conditions.

6. Conclusion

The impact of vehicles' movement on the dispersion of pollution in the street canyon is characterized into two aspects: 1) the VIT effect, that is, the movement of the vehicles changes the vortex structure of flow field in the street canyon; 2) the vehicle exhaust pollutants. The previous research mainly studied the role of one of the two aspects separately rather than studied the coupling effect of these two aspects. Considering the influence of the above two aspects, this paper simulates the vehicle movement in actual street canyon and visualizes the exhaust emission process of the moving vehicles by using dynamic mesh updating method, which provides a novel method for studying the VIT effect and vehicular pollution in the street canyon.

The simulation results show that the vehicles arrangement plays a crucial role in the dispersion of exhaust pollution. When vehicles are moving in staggered arrangement, the distribution of their vehicular pollution is more uniform than that of the vehicles moving in-line arrangement. Both vehicle speed and ambient wind velocity have important effects on pollution dispersion in street canyon. High-speed vehicles can enhance the turbulence, make vehicular pollutants spread more evenly, but have little impact on overall levels of pollution in street canyon. However, the variations of ambient wind velocity are able to change the flow field and exhaust jet plume in the street canyon, and determine the pollution concentration within the street canyon. With increasing the ambient wind velocity, the exposure level of pedestrian on the street decreases, especially on the windward side. With increasing the distance and extending the time of vehicle movement, it has been found out that the time for reaching the stable state of the dispersion of VIT and exhaust pollutants in the wake of constant speed vehicles is approximately 7s. Based on the range of exhaust emissions dispersion in vehicle wake at stable state, a "healthy distance" of 8 m is proposed to remind the drivers to avoid the direct influence of the surrounding vehicles exhaust. At last, according to the influence range of the VIT if the vehicle is running at steady status, the VIT can be regarded as a continuous turbulence source when the vehicles travel with a "safe distance" on the road to form a stable traffic flow.

Declaration of competing interest

The authors declare that they have no known competing financial interests or personal relationships that could have appeared to influence the work reported in this paper.

Acknowledgments

This study was financially supported by the National Natural Science Foundation of China (Grant No. 51778511, 51778253), the Hubei Provincial Natural Science Foundation of China (Grant No. 2018CFA029), the Key Project of ESI Discipline Development of Wuhan University of Technology (WUT Grant No. 2017001), and the Fundamental Research Funds for the Central Universities (WUT Grant No. 2019IVB082).

References

[1] China National Economic and Social Development Statistics Bulletin 2019, 2019.
[2] T.R. Gong, T.Z. Ming, X.M. Huang, R. De Richter, Y.J. Wu, W. Liu, Numerical analysis on a solar chimney with an inverted U-type cooling tower to mitigate urban air pollution, Sol. Energy 147 (MAY) (2017) 68–82.
[3] F. Xue, X.F. Li, The Impact of Roadside Trees on Traffic Released PM10 in Urban Street Canyon: Aerodynamic and Deposition Effects, Sustainable Cities & Society, 2017.
[4] K. Niachou, I. Livada, M. Santamouris, Experimental study of temperature and airflow distribution inside an urban street canyon during hot summer weather conditions—Part I: air and surface temperatures, Build. Environ. 43 (8) (2008) 1383–1392.
[5] J. Allegrini, V. Dorer, J. Carmeliet, Wind tunnel measurements of buoyant flows in street canyons, Build. Environ. 59 (JAN) (2013) 315–326.
[6] J. Hang, M. Sandberg, Y.G. Li, L. Claesson, Pollutant dispersion in idealized city models with different urban morphologies, Atmos. Environ. 43 (38) (2009) 6011–6025.
[7] J. Hang, Y.G. Li, M. Sandberg, R. Buccolieri, S.D. Sabatino, The influence of building height variability on pollutant dispersion and pedestrian ventilation in idealized high-rise urban areas, Build. Environ. 56 (2012) 346–360.
[8] Q.K. Wang, W.J. Fang, R.D. Richter, C. Peng, T.Z. Ming, Effect of moving vehicles on pollutant dispersion in street canyon by using dynamic mesh updating method, J. Wind Eng. Ind. Aerod. 185 (2019) 15–25.
[9] F. Ali-Toudert, H. Mayer, Numerical study on the effects of aspect ratio and orientation of an urban street canyon on outdoor thermal comfort in hot and dry climate, Build. Environ. 41 (2) (2006) 94–108.
[10] Z. Baratian-Ghorghi, N.B. Kaye, The effect of canyon aspect ratio on flushing of dense pollutants from an isolated street canyon, Sci. Total Environ. 443 (3) (2013) 112–122.
[11] Y.H. Juan, A.S. Yang, C.Y. Wen, Y.T. Lee, P.C. Wang, Optimization procedures for enhancement of city breathability using arcade design in a realistic high-rise urban area, Build. Environ. 121 (aug) (2017) 247–261.
[12] R.A. Memon, D.Y.C. Leung, C.H. Liu, Effects of building aspect ratio and wind speed on air temperatures in urban-like street canyons, Build. Environ. 45 (1) (2010) 176–188.
[13] T.R. Oke, Street design and urban canopy layer climate, Energy Build. 11 (1) (1988) 103–113.
[14] C.R. Hao, X.M. Xie, Y. Huang, Z. Huang, Study on influence of viaduct and noise barriers on the particulate matter dispersion in street canyons by CFD modeling, Atmospheric Pollution Research 10 (6) (2019) 1723–1735.
[15] J. Hang, R. Buccolieri, X. Yang, H.Y. Yang, F. Quarta, B.M. Wang, The impacts of viaduct settings and street aspect ratios on personal intake fraction in three-dimensional urban-like geometries, Build. Environ. 143 (2018) 138–162.

[16] D.J. Nowak, D.E. Crane, J.C. Stevens, Air pollution removal by urban trees and shrubs in the United States, Urban For. Urban Green. 4 (3–4) (2006) 115–123.
[17] J.W. Su, L. Wang, Z.L. Gu, M.M. Song, Z.R. Cao, Effects of real trees and their structure on pollutant dispersion and flow field in an idealized street canyon, Atmospheric Pollution Research 10 (6) (2019) 1699–1710.
[18] C. Lup, N. Negin, N. Leslie, Pedestrian-level urban wind flow enhancement with wind catchers, Atmosphere 8 (12) (2017) 159.
[19] Z.T. Li, T.H. Shi, Y.J. Wu, X.M. Huang, Y.H. Juan, T.Z. Ming, N. Zhou, Effect of traffic tidal flow on pollutant dispersion in various street canyons and corresponding mitigation strategies, Energy and Built Environment 1 (3) (2020) 242–253.
[20] J.W.D. Boddy, R.J. Smalley, N.S. Dixon, J.E. Tate, A.S. Tomlin, The spatial variability in concentrations of a traffic-related pollutant in two street canyons in York, UK—Part I: the influence of background winds, Atmos. Environ. 39 (17) (2005) 3147–3161.
[21] C. Gromke, R. Buccolieri, S.D. Sabatino, B. Ruck, Dispersion study in a street canyon with tree planting by means of wind tunnel and numerical investigations – evaluation of CFD data with experimental data, Atmos. Environ. 42 (37) (2008) 8640–8650.
[22] J.J. Kim, J.J. Baik, A numerical study of the effects of ambient wind direction on flow and dispersion in urban street canyons using the RNG k-ε turbulence model, Atmos. Environ. 38 (19) (2004) 3039–3048.
[23] P. Moonen, V. Dorer, J. Carmeliet, Evaluation of the Ventilation Potential of Courtyards and Urban Street Canyons Using RANS and LES, vol. 99, 2011, pp. 414–423, 4.
[24] D.M. Hargreaves, C.J. Baker, Gaussian puff model of an urban street canyon, J. Wind Eng. Ind. Aerod. (1997) 927–939.
[25] H. Huang, A. Yoshiaki, A. Mitsuru, T. Masamitsu, A two-dimensional air quality model in an urban street canyon: evaluation and sensitivity analysis, Atmos. Environ. 34 (5) (2000) 689–698.
[26] X.M. Xie, H. Zhen, J.S. Wang, Z. Xie, Thermal effects on vehicle emission dispersion in an urban street canyon, Transport. Res. Transport Environ. 10D (3) (2005) 197–212.
[27] R.E. Eskridge, J.C.R. Hunt, Highway modeling. Part I: prediction of velocity and turbulence fields in the wake of vehicles, Journal of Applied Meteorology & Climatology 18 (4) (1979) 387–400.
[28] Z.E. Hider, S. Hibberd, C.J. Baker, Modelling particulate dispersion in the wake of a vehicle, J. Wind Eng. Ind. Aerod. s 67–68 (97) (1997) 733–744.
[29] Y. Qin, S.C. Kot, Dispersion of vehicular emission in street canyons, Guangzhou City, South China (P.R.C.), Atmos. Environ. Part B - Urban Atmos. 27 (3) (1993) 283–291.
[30] G. Vachon, P. Louka, J.M. Rosant, P.G. Mestayer, J.F. Sini, Measurements of traffic-induced turbulence within a street canyon during the Nantes'99 experiment, Water Air Soil Pollut. Focus 2 (5) (2002) 127–140.
[31] P. Kastner-Klein, E. Fedorovich, M.W. Rotach, A wind tunnel study of organised and turbulent air motions in urban street canyons, J. Wind Eng. Ind. Aerod. 89 (9) (2001) 849–861.
[32] P. Kastnerklein, E. Fedorovich, M. Ketzel, R. Berkowicz, R. Britter, The modelling of turbulence from traffic in urban dispersion models — Part II: evaluation against laboratory and full-scale concentration measurements in street canyons, Environ. Fluid Mech. 3 (2) (2003) 145–172.
[33] S.D. Sabatino, P. Kastner-Klein, R. Berkowicz, R.E. Britter, E. Fedorovich, The modelling of turbulence from traffic in urban dispersion models – Part I: theoretical considerations, Environ. Fluid Mech. 3 (2) (2003) 129–143.
[34] K. Ahmad, M. Khare, K.K. Chaudhry, Model vehicle movement system in wind tunnels for exhaust dispersion studies under various urban street configurations, J. Wind Eng. Ind. Aerod. 90 (9) (2002) 1051–1064.
[35] U. Bhautmage, S. Gokhale, Effects of moving-vehicle wakes on pollutant dispersion inside a highway road tunnel, Environ. Pollut. 218 (2016) 783–793.
[36] P. Thaker, S. Gokhale, The impact of traffic-flow patterns on air quality in urban street canyons, Environ. Pollut. 208 (JAN.PT.A) (2016) 161–169.
[37] Y.W. Zhang, Z.L. Gu, C.W. Yu, Large eddy simulation of vehicle induced turbulence in an urban street canyon with a new dynamically vehicle-tracking scheme, Aerosol & Air Quality Research 17 (3) (2017) 865–874.
[38] Z.T. Li, J. Xu, T.Z. Ming, C. Peng, J.Y. Huang, Numerical simulation on the effect of vehicle movement on pollutant dispersion in urban street, Procedia Engineer 205 (2017) 2303–2310.
[39] C.J. Cai, T.Z. Ming, W.J. Fang, R.D. Richter, C. Peng, The Effect of Turbulence Induced by Different Kinds of Moving Vehicles in Street Canyons, vol. 54, Sustainable Cities and Society, 2020, 102015.
[40] Z.M. Tong, Y.J. Chen, A. Malkawi, G. Adamkiewicz, J.D. Spengler, Quantifying the impact of traffic-related air pollution on the indoor air quality of a naturally ventilated building, Environ. Int. 89–90 (2016) 138–146.
[41] G. Dong, T.L. Chan, Large eddy simulation of flow structures and pollutant dispersion in the near-wake region of a light-duty diesel vehicle, Atmos. Environ. 40 (6) (2006) 1104–1116.
[42] X.J. Hu, H.B. Yang, B. Yang, X.C. Li, Y.L. Lei, Effect of Car Rear Shape on Pollution Dispersion in Near Wake Region, 2015.
[43] Z. Ning, C.S. Cheung, Y. Lu, M.A. Liu, W.T. Hung, Experimental and numerical study of the dispersion of motor vehicle pollutants under idle condition, Atmos. Environ. 39 (40) (2005) 7880–7893.
[44] J. Hang, Z.W. Luo, X.M. Wang, L.J. He, B.M. Wang, W. Zhu, The influence of street layouts and viaduct settings on daily carbon monoxide exposure and intake fraction in idealized urban canyons, Environ. Pollut. 220 (2017) 72–86.
[45] L.J. He, J. Hang, X.M. Wang, B.R. Lin, X.H. Li, G. D Lan, Numerical investigations of flow and passive pollutant exposure in high-rise deep street canyons with various street aspect ratios and viaduct settings, Sci. Total Environ. 584 (2017) 189–206.
[46] Z.W. Luo, Y.G. Li, W.W. Nazaroff, Intake fraction of nonreactive motor vehicle exhaust in Hong Kong, Atmos. Environ. 44 (15) (2010) 1913–1918.
[47] China National Economic and Social Development Statistics Bulletin 2018, 2018.
[48] M. Allan, G.M. Richardson, H. Jones-Otazo, Probability density functions describing 24-hour inhalation rates for use in human health risk assessments: an update and comparison, Human and Ecological Risk Assessment 14 (2) (2008) 372–391.
[49] C. K Chau, E.Y. Tu, D.W. T Chan, J. Burnett, Estimating the total exposure to air pollutants for different population age groups in Hong Kong, Environ. Int. 27 (8) (2002) 617–630.
[50] X.M. Xie, Z. Huang, J.S. Wang, The impact of urban street layout on local atmospheric environment, Build. Environ. 41 (10) (2006) 1352–1363.
[51] X.X. Li, C.H. Liu, D.Y.C. Leung, K.M. Lam, Recent progress in CFD modelling of wind field and pollutant transport in street canyons, Atmos. Environ. 40 (29) (2006) 5640–5658.
[52] Z.L. Gu, Y.W. Zhang, Y. Cheng, S.C. Lee, Effect of uneven building layout on air flow and pollutant dispersion in non-uniform street canyons, Build. Environ. 46 (12) (2011) 2657–2665.
[53] T.Z. Ming, W.J. Fang, C. Peng, C.J. Cai, R.D. Richter, M.H. Ahmadi, Y.G. Wen, Impacts of traffic tidal flow on pollutant dispersion in a non-uniform urban street canyon, Atmosphere 9 (3) (2018) 82.
[54] T.L. Chan, G. Dong, C.W. Leung, C.S. Cheung, Validation of a two-dimensional pollutant dispersion model in an isolated street canyon, Atmos. Environ. 36 (5) (2002) 861–872.
[55] X.X. Li, C.H. Liu, D.Y.C. Leung, Development of a k—ε model for the determination of air exchange rates for street canyons, Atmos. Environ. 39 (38) (2005) 7285–7296.
[56] N.M. Sudharsan, R. Ajaykumar, K. Murali, K. Kumar, A comparative study of dynamic mesh updating methods used in the simulation of fluid-structure interaction problems with a non-linear free surface, 1989-1996, ARCHIVE Proceedings of the Institution of Mechanical Engineers Part C Journal of Mechanical Engineering Science 203–210 (3) (2004) 283–300, 218.
[57] ANSYS Fluent 19 Tutorial Guide.
[58] W. Xiong, C.S. Cai, B. Kong, X. Kong, CFD simulations and analyses for bridge-scour development using a dynamic-mesh updating technique, J. Comput. Civ. Eng. 30 (1) (2016), 04014121.
[59] J. Zhong, X.M. Cai, W.J. Bloss, Coupling dynamics and chemistry in the air pollution modelling of street canyons: a review, Environ. Pollut. 214 (2016) 690–704.
[60] H.J. Wang, Q.Y. Chen, A new empirical model for predicting single-sided, wind-driven natural ventilation in buildings, Energy Build. 54 (NOV) (2012) 386–394.